PHYSICAL REVIEW D **95,** 126005 (2017)

Interplay of Reggeon and photon in *pA* collisions

Gokce Basar,[1,*] Dmitri E. Kharzeev,[2,3,4,†] Ho-Ung Yee,[1,4,‡] and Ismail Zahed[2,§]

[1]*Department of Physics, University of Illinois, Chicago, Illinois 60607, USA*
[2]*Department of Physics and Astronomy, Stony Brook University, Stony Brook, New York 11794-3800, USA*
[3]*Department of Physics, Brookhaven National Laboratory, Upton, New York 11973-5000, USA*
[4]*RIKEN-BNL Research Center, Brookhaven National Laboratory, Upton, New York 11973-5000, USA*

(Received 12 April 2017; published 14 June 2017)

We discuss the effects of the electromagnetic interaction in high-energy proton collisions with nuclei of large Z at strong coupling $\lambda = g^2 N_c$. Using the holographic dual limit of large $N_c > \lambda \gg 1$, we describe the Reggeon exchange as a twisted surface and show that it gets essentially modified by the electromagnetic interaction.

DOI: 10.1103/PhysRevD.95.126005

I. INTRODUCTION

High-energy diffractive hadron interactions with a large rapidity gap $\chi = \ln(s/s_0)$ are dominated by the Reggeon and Pomeron exchanges. In pp scattering the Reggeon exchange is dominant below $\sqrt{s} = 5$ GeV, while the Pomeron exchange dominates at higher $\sqrt{s}$ [1]. At weak coupling, the Pomeron and Reggeon exchanges are described by rapidity ordered Balitsky-Fadin-Kuraev-Lipatov ladder diagrams [2]. The effects of the electromagnetic interaction are usually assumed to be weak.

At strong t'Hooft coupling $\lambda = g^2 N_c$, the Pomeron and Reggeon exchanges have been addressed in the context of holography with and without supersymmetry by a number of authors [3–21]. Since QCD is not supersymmetric, the Reggeon and Pomeron are best described by surface exchanges with nonsupersymmetric holographic metric, whereby the massless spin-2 graviton transmutes to a massive spin-2 glueball and decouple in the pertinent kinematics [4,5,16,17,19–21]. The surface exchanges are noteworthy as they encode a stringy Schwinger mechanism [16], which is also present when the surface extrinsic curvature is included [22]. They play an important role in the initial conditions for both saturation [23] and prompt thermalization [24,25].

Our analysis below makes use of the holographic picture of Reggeon exchange initially discussed in [5], with a particular focus on the role of electromagnetic corrections in *pA* collisions with a large Z nucleus. The dedicated pA experiments at the LHC and RHIC colliders using heavy nuclei may access the physics that we detail below. In Sec. II, we review the analysis of the Reggeon amplitude at strong coupling using a semiclassical surface analysis. In Sec. III, we show how the effects of photon exchange modify the semiclassical analysis. Our conclusions follow in Sec. IV.

II. REGGEON AMPLITUDES IN STRONG COUPLING

In this section, we give a brief review of the framework for computing Reggeon amplitudes in strong coupling, following the work of Ref. [5]. The motivation of the setup comes from the AdS/CFT correspondence or holographic QCD, where a strongly coupled, large N_c gauge theory may be described by a dual string theory in a holographic five-dimensional space-time. The extra holographic dimension represents an energy scale of the problem, so that it can be thought of as a geometric realization of renormalization group flow between different energy scales. The five-dimensional physics around the UV region of the holographic coordinate should correspond to the UV physics of the dual field theory, and it is geometrically separated from the physics of the IR scales that are happening in the IR region of the holographic coordinate. This "locality" in energy scales seems to be an important peculiarity that holds in the strongly coupled, large N_c gauge theory which has a holographic dual description [26]. We assume that the large N_c QCD in its low-energy regime is one such theory, or more conservatively we expect that a proper dual five-dimensional theory may capture important physics of large N_c QCD in its low-energy, strongly coupled regime. Extending the results from large N_c to $N_c = 3$ is according to the usual spirit of considering the large N_c approximation.

We are interested in the high-energy scattering with a low momentum transfer, $(-t) \equiv -q^2 \ll \Lambda_{\rm QCD}^2$, or equivalently with a large impact parameter $b \gg \Lambda_{\rm QCD}^{-2}$. Although the center of mass energy $\sqrt{s}$ is much larger than the QCD scale, the physics governing this scattering process is in the regime of low energy, set by the momentum transfer $\sqrt{-t} \ll \Lambda_{\rm QCD}$, and it is nonperturbative, strongly coupled, warranting the application of ideas of AdS/CFT correspondence or holography. There have been several works in this

*basar@uic.edu
†dmitri.kharzeev@stonybrook.edu
‡hyee@uic.edu
§ismail.zahed@stonybrook.edu

direction for both Pomeron and Reggeon exchanges [3,4,6,8,9,12–18]. Here, we distinguish the amplitudes with Reggeon exchanges from those with Pomerons by the fact that Reggeons carry nonzero quantum numbers of the quark flavor symmetry whereas Pomerons have vacuum quantum numbers. A Reggeon then necessarily consists of at least a valence quark and an antiquark pair in its wave function, something like a flavored meson. On the other hand, one may expect that Pomerons are dominantly made of colorless, flavorless glueballs. This naturally maps Reggeons to the holographic degrees of freedom describing flavored mesons (such as the five-dimensional fields living on the "probe branes" representing quark dynamics), and Pomerons to the bulk degrees of freedom corresponding to glueball dynamics. The problem of high-energy scattering in strong coupling would then be transformed to a scattering of the appropriate five-dimensional degrees of freedoms in the holographic dual five-dimensional space-time: for Reggeons, it is an open string exchange amplitude, whereas for Pomerons, it would be a closed string amplitude. Generally speaking, computing these amplitudes in a curved space-time such as the holographic dual space-time is hard and not well known. Various attempts with useful and meaningful approximations have been performed, which gave us a fairly good, but still incomplete understanding on these amplitudes. Since the description is supposed to capture full nonperturbative dynamics of QCD, the results should, in principle, satisfy all known consistency theorems such as the Froissart bound on the total cross section [27].

We follow the approximation introduced in Ref. [5] in our study of possible interplay between Reggeons and QED photons. The idea of Ref. [5] is to approximate the full stringy amplitude with its semiclassical saddle point contribution. This approximation can be well justified in the framework of holography where the string world-sheet action is proportional to the large t'Hooft coupling factor $\sim\sqrt{\lambda}$ ($\lambda \equiv g_{\rm YM}^2 N_c$) warranting the use of semiclassical approximation. Moreover, it has been known that the high s, small t regime of string amplitudes is generically governed by semiclassical world-sheet configurations, even without explicit strong coupling enhancement [28]. Based on this, one may expect that the semiclassical approximation captures the main ingredients of the scattering amplitudes in the high s, small t regime. Reference [5] was able to describe the Regge behavior of the scattering amplitudes,

$$\mathcal{T} \sim i s^{\alpha_0+\alpha' t}, \tag{2.1}$$

within this approximation.

We make a further approximation assuming that most of the string world sheets in the semiclassical solutions reside at the IR bottom of the holographic coordinate with an effective string tension $T_{\rm eff} = \frac{1}{2\pi\alpha'}$. In the regime of interest $(-t) > 0$ (spacelike momentum transfer), the validity of this approximation is model dependent as first discussed in Ref. [8] (see also Ref. [16]). There is a general tendency of pushing the string world sheets toward a more UV region when $(-t) > 0$ whereas there is a competing gravitational attraction toward the IR region. The former is proportional to $(-t)$ while the latter is independent of $(-t)$, so that for some moderate values of $(-t)$ the string world sheets can indeed stay near the IR bottom in a model-dependent way. Since we are focusing on very small values of $(-t)$ [in fact, $(-t) = 0$ when we discuss the total cross section using the optical theorem], this locality to the IR bottom may well be justified. We should emphasize however that it would certainly be possible to include diffusion dynamics along the holographic coordinate beyond this approximation, in a similar way to those done for the Pomeron amplitudes in Refs. [8,13,17,18].

The kinematics of a Reggeon exchange amplitude is depicted in Fig. 1. Two projectiles carrying valence quarks or antiquarks exchange a pair of quark-antiquark pairs during the collision process. In the high-energy limit, the spectators other than the exchanged quark-antiquark pair travel straight without much modification in their trajectories, and one can simply assume that their trajectories are not modified at all in the eikonal approximation. The QCD in the strongly coupled, confined regime results in configurations of QCD flux tubes (strings) joining the exchanged quark-antiquark pair, so that the space-time picture of the string world sheet is a two-dimensional surface with its boundaries being the world lines of the exchanged quark antiquarks. The full string amplitude of this open string exchange is obtained by summing over all configurations of string world sheets with the boundaries given by the world lines of the exchanged pair. Note that

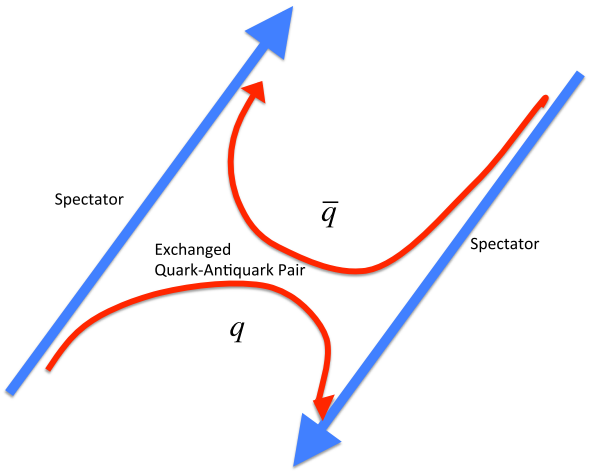

FIG. 1. Kinematics of a Reggeon exchange scattering in the high-energy eikonal limit. Spectators move straight without deflection, while a quark-antiquark pair is exchanged. A two-dimensional open string world sheet with the boundary set by the trajectories of the exchanged quark-antiquark pair describes the amplitude.

these boundaries, or the world lines of the exchanged quark-antiquark pair, are dynamical, so that the path integral of string configurations includes the variation of the boundaries too. The asymptotic trajectories in the infinite past and the future, coinciding with the eikonalized spectator trajectories, set the boundary condition for this variational problem. Note that while a Pomeron amplitude, which is described as a dipole-dipole scattering, can be reduced to a connected expectation value of two Wilson loops in the eikonal limit [29], our Reggeon amplitude, which involves an exchange of dynamical quark-antiquark pairs, cannot simply be reduced to Wilson lines/loops. The task at hand is precisely equal to computing an open string amplitude, except the somewhat unconventional incoming/outgoing states specified in the real space-time rather than in the momentum space. We approximate this amplitude with a semiclassical contribution obtained by finding an extremum solution of the classical Nambu-Goto string action with the specified asymptotic boundary condition.

As in Ref. [5] we compute the amplitude in the Euclidean space and analytically continue the result to the Minkowski space-time. The rapidity difference $\chi = \log s$ in the Minkowski space becomes an angle $\theta = -i\chi$ on the longitudinal plane in the Euclidean space [30] between the two asymptotic trajectories of the projectiles. The two asymptotic trajectories have an impact parameter b in the transverse plane. After identifying the dominant semiclassical configuration, the amplitude $\mathcal{T}(s,b)$ in the impact parameter space then is given by

$$\frac{\mathcal{T}(s,b)}{2is} \sim \frac{1}{s}\exp\left[-S_{\text{saddle}}(\theta \to -i\chi)\right], \tag{2.2}$$

where the $\frac{1}{s}$ in front is the spin factor arising from the Berry phase of the exchanged Dirac spinors in high-energy limit [5], and S_{saddle} is the classical Nambu-Goto string action evaluated on the extremum solution. The t-space amplitude $\mathcal{T}(s,t)$ is related to $\mathcal{T}(s,b)$ by the Fourier transform,

$$\mathcal{T}(s,t) = \int d^2b e^{iq\cdot b}\mathcal{T}(s,b), \qquad t \equiv -q^2. \tag{2.3}$$

Note that with our definition of the amplitude $\mathcal{T}$ as above, the total cross section via the optical theorem is given by

$$\begin{aligned}\sigma_{\text{tot}} &= \frac{1}{s}\text{Im}\mathcal{T}(s,t=0) = \frac{1}{s}\int d^2b \text{Im}\mathcal{T}(s,b) \\ &= \frac{2}{s}\int d^2b \text{Re}(e^{-S_{\text{saddle}}(\theta\to -i\chi)})(b),\end{aligned} \tag{2.4}$$

which we use later.

Let the longitudinal plane be parametrized by (x^0, x^3) and the world line of the first projectile be given by $(x^0, x^3) = (\tau, 0)$ $(-\infty < \tau < \infty)$, sitting at the origin of the transverse plane spanned by (x^1, x^2). The world line of the second projectile has a relative angle θ in the longitudinal plane, so that $(x^0, x^3) = (\tau\cos\theta, \tau\sin\theta)$ $(-\infty < \tau < \infty)$, and is separated by a distance b in the transverse plane $(x^1, x^2) = (b, 0)$. We have to find the open string extremum whose asymptotic boundaries are specified by these two world lines (see Fig. 2). Near each trajectory, the string world sheet tends to be parallel to the above straight lines, and since these two world lines have a relative angle θ with a distance b, the string world sheet has to twist itself on the longitudinal plane as it spans the transverse direction along x^1 of distance b to connect the two world lines. It is natural to expect that to a good approximation the string world sheet that minimizes its area lies close to the helicoidal surface bounded by the above two world lines,

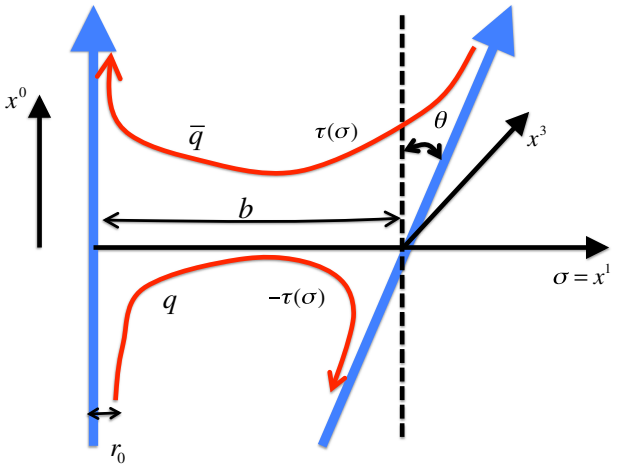

FIG. 2. Euclidean configuration of a high-energy Reggeon scattering. The two spectator trajectories have a relative angle θ in the longitudinal plane (x^0, x^3), and are separated by an impact parameter b in the transverse plane (x^1, x^2). The exchanged quark-antiquark pair world lines reside on the helicoid spanned between these two straight lines of the spectators, and are parametrized by a single function $\tau(\sigma)$.

$$\begin{aligned}x^\mu(\sigma,\tau):\ &(x^0 = \tau\cos(\theta(\sigma)), x^3 = \tau\sin(\theta(\sigma)),\\ &x^1 = \sigma, x^2 = 0), \qquad \theta(\sigma) \equiv \frac{\theta}{b}\sigma,\end{aligned} \tag{2.5}$$

where the surface coordinates span $0 < \sigma < b$ and $-\infty < \tau < \infty$. This was pointed out in Ref. [5] and was successfully used to reproduce the leading Regge trajectory expected from the high-energy limit of the open string Veneziano amplitude. The open string world sheet on this helicoid surface corresponding to a Reggeon exchange is specified by its two boundary curves on the helicoid surface joining the two straight world lines, as these curves represent the world lines of the exchanged quark and antiquark pair. One can parametrize these curves in the helicoid surface coordinates (σ, τ) by a single function $\tau(\sigma)$ $(0 < \sigma < b)$,

$$(\sigma,\tau)=(\sigma,\pm\tau(\sigma)), \tag{2.6}$$

where the two curves differ simply by a sign of τ coordinate due to an obvious symmetry $\tau\to-\tau$. See Fig. 2 for details. The open string world sheet therefore covers a part of helicoid surface specified by the coordinate range $0<\sigma<b$ and $-\tau(\sigma)<\tau<\tau(\sigma)$, with yet to be determined function $\tau(\sigma)$ by extremizing the Nambu-Goto action. The Nambu-Goto action is easily found to be

$$S_{\text{Reggeon}}=\frac{1}{2\pi\alpha'}\int_0^b d\sigma\int_{-\tau(\sigma)}^{\tau(\sigma)}d\tau\sqrt{1+\frac{\theta^2}{b^2}\tau^2}. \tag{2.7}$$

It is convenient to perform the analytic continuation $\theta\to-i\chi$ at this point to obtain

$$S_{\text{Reggeon}}=\frac{1}{2\pi\alpha'}\int_0^b d\sigma\int_{-\tau(\sigma)}^{\tau(\sigma)}d\tau\sqrt{1-\frac{\chi^2}{b^2}\tau^2}, \tag{2.8}$$

whereas we do not need to analytically continue the τ variable as it is just an integration variable.[1] Extremizing the above gives an equation of motion

$$1-\frac{\chi^2}{b^2}\tau(\sigma)^2=0, \tag{2.9}$$

with the trivial solution $\tau(\sigma)=\frac{b}{\chi}$, whose on-shell action is

$$S_{\text{saddle}}=\frac{1}{2\pi\alpha'}\int_0^b d\sigma\int_{-\frac{b}{\chi}}^{\frac{b}{\chi}}d\tau\sqrt{1-\frac{\chi^2}{b^2}\tau^2}=\frac{b^2}{4\alpha'\chi}. \tag{2.10}$$

The resulting t-space amplitude is then given by

$$\begin{aligned}\mathcal{T}(s,t)&\sim 2i\int_0^\infty bdb\int_0^{2\pi}d\theta e^{i\sqrt{(-t)}b\cos\theta}e^{-\frac{b^2}{4\alpha'\chi}}\\&\sim i(\log s)s^{\alpha' t},\end{aligned} \tag{2.11}$$

which shows the expected Regge behavior for Reggeon amplitudes [5]. In the next section, we use this computational framework developed in Ref. [5] to study the interesting interplay between Reggeons and QED photons in the regime where QED interactions can no longer be neglected due to a large $Z\sim 100$ enhancement for heavy ions.

III. INTERPLAY OF REGGEON AND PHOTON IN pA COLLISIONS

Within the framework of the previous section, we now include the QED interactions and establish how the QCD Reggeon dynamics is affected by them. There are two points that we have to emphasize. The first thing is that the effect we are discussing is not a mere quantum mechanical interference between Reggeon and QED amplitudes when we square the total amplitude to obtain the cross section. Rather, we are studying effects that modify Reggeon and QED amplitudes themselves due to an interplay between the two. This clearly contrasts to the case of Pomerons, where the QED interactions do not affect Pomeron amplitudes *per se* and the only effects one sees are the interference of mutually independent Pomeron and QED amplitudes in the cross sections. The difference between Pomerons and Reggeons in this aspect is due to the fact that Reggeons are in general charged under QED interactions whereas Pomerons are neutral. This point becomes clearer as we go on. The second point we emphasize is about the magnitude of the QED interactions in the problem. Previous works have ignored QED effects in computing Reggeon amplitudes relying on the smallness of α_{EM} compared to the strong QCD interactions. This assumption however fails in our problem due to a large $Z\sim 100$ enhancement in pA collisions, and one should take care of QED interactions properly in computing the full Reggeon and QED amplitudes.

We follow the same variational approach to the problem as described in the previous section. The trajectories of the exchanged quark-antiquark pair are assumed to be on the helicoid surface between the spectator trajectories. See Fig. 3 for the geometry and definitions of our problem. One difference is that in our case, the upper (quark) and lower (antiquark) trajectories are not necessarily symmetric with respect to time inversion $\tau\to-\tau$ when their QED charges are not equal in magnitude, so one has to introduce two

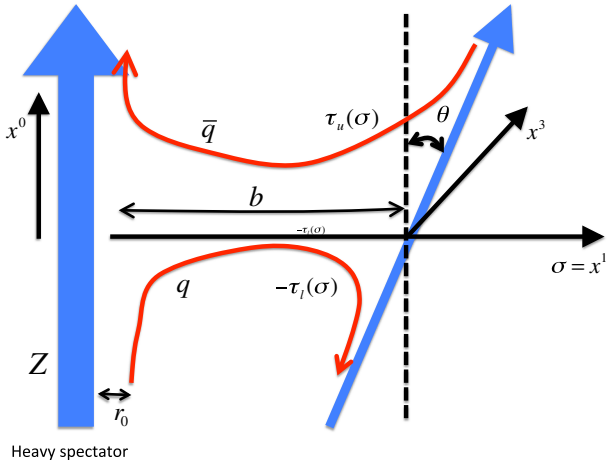

FIG. 3. Euclidean configuration of Reggeon exchange scattering between a heavy ion with a charge Z and a proton. Definitions are the same as in Fig. 2, except that the exchanged quark-antiquark trajectories are parametrized by two independent functions $\tau_u(\sigma)$ and $\tau_d(\sigma)$. We include QED interactions between the charge Z spectator and the rest of the particles in the leading large Z approximation.

[1]However, the solutions should be related by the analytic continuation, $\tau(\sigma)\to i\tau(\sigma)$.

separate functions $\tau_{u,d}(\sigma)$ to parametrize upper/lower trajectories. The range of world sheet time τ for the string world sheet bounded by exchanged quark-antiquark pair would then be

$$-\tau_d(\sigma) \le \tau \le \tau_u(\sigma). \tag{3.1}$$

The nonperturbative QCD contribution (Reggeon contribution) to the action is as before

$$S_{\text{Reggeon}} = \frac{1}{2\pi\alpha'}\int_0^b d\sigma \int_{-\tau_d(\sigma)}^{\tau_u(\sigma)} d\tau \sqrt{1+\frac{\theta^2}{b^2}\tau^2}. \tag{3.2}$$

The QED part of the amplitude is simply the QED expectation value of the Wilson lines for charged particle trajectories weighted by their charges. In the leading large Z approximation we are taking, the computation simplifies drastically by the fact we only include mutual interactions between the charge Z spectator and the rest particles. In the approximation of neglecting the dynamical quark-antiquark loop for the photon propagator, the QED becomes a free theory of photons and the semiclassical treatment of Wilson line expectation values becomes exact. In other words, the connected expectation value of multiple Wilson lines given by curves C_i,

$$\frac{\langle \prod_i W(C_i)\rangle}{\prod_i \langle W(C_i)\rangle}, \tag{3.3}$$

is given by a product of connected expectation values of pairs of Wilson lines,

$$\prod_{i\neq j} W_{ij}, \qquad W_{ij} \equiv \frac{\langle W(C_i)W(C_j)\rangle}{\langle W(C_i)\rangle\langle W(C_j)\rangle}. \tag{3.4}$$

Also, W_{ij} is computed simply by the semiclassical expression

$$W_{ij} = e^{iq_i e\int_{C_i} A_j^\mu dx_\mu} = e^{iq_j e\int_{C_j} A_i^\mu dx_\mu}, \tag{3.5}$$

where A_i is the classical solution of Maxwell's equation sourced by the curve C_i with charge q_i.

In leading Z approximation we only have to compute W_{ij} with i being equal to the charge Z spectator, and it is sufficient to know the semiclassical A_μ sourced by the trajectory of the charge Z spectator which is a straight line in (Euclidean) space-time in the high-energy eikonal approximation. Working in the rest frame of the charge Z spectator for convenience where it is located at spatial origin of the coordinate traveling straight along the (Euclidean) time, the solution is[2]

$$A_0 = i\frac{Ze}{4\pi r}, \qquad r=\sqrt{\vec{x}\cdot\vec{x}}, \qquad \vec{A}=0, \tag{3.6}$$

and the total QED amplitude in leading Z approximation reads as

$$\exp\left[ie\sum_i q_i\int_{C_i} A_\mu dx^\mu\right] \equiv \exp\left[-S_{\text{QED}}\right], \tag{3.7}$$

where i runs over the rest of the charged particles. Without an interplay with the Reggeon contribution (3.2), the QED amplitude in (3.7) would simply be a pure phase after analytic continuation to the Minkowski signature. As we observe shortly, the interplay with Reggeons can in general make the QED amplitude develop modulus change, that is, a nonzero real part in S_{QED}.

It is easy to compute S_{QED} by integrating (3.6) over the trajectories of the rest particles. See Fig. 3 for a pictorial explanation of the charged particle trajectories. In the asymptotic past, one of the two incoming projectiles is a bound state of a charge Z spectator and a charge q_d quark, and the latter is exchanged with the other incoming projectile which comprises a charge $-q_d$ antiquark and the spectator particle of charge q. We assume that inside the bound state, the charge Z spectator and the charge q_d quark are separated by a small distance r_0 which serves as a regularization of S_{QED} between the two. Our results are not sensitive to r_0. Phenomenologically it would be reasonable to take $r_0 = 1$ fm. A small separation between the charge $-q_d$ antiquark and the charge q spectator in the other projectile is easily seen to be irrelevant and is ignored. The same is true for the internal sizes of the charge Z spectator and charge q spectator, and we treat them as pointlike. In the asymptotic future, the outgoing projectiles are a bound state of a charge Z spectator and a charge q_u quark that has been exchanged, and a bound state of a charge q spectator and a charge $-q_u$ antiquark. We take the same assumption on the internal separation of constituents particles inside the bound states as in the asymptotic past.

We are only interested in the part of S_{QED} that depends on the trajectories of the exchanged quark-antiquark pair given by two functions $\tau_{u,d}(\sigma)$, because we perform a saddle point approximation in integrating over those trajectories. We therefore will not consider the charge q spectator in the following.[3] The charge q_d quark (or equivalently the charge $-q_d$ antiquark) trajectory given by $\tau_d(\sigma)$ (the lower trajectory in Fig. 3) gives the contribution to S_{QED} as

[2]We are working in Euclidean signature, and then analytically continue to Minkowski space-time by $\theta \to -i\chi$, and $x^0 \to it$, where χ is space-time rapidity which should be roughly equal to the kinematic rapidity $\log(\frac{s}{m^2})$.

[3]Its contribution to the amplitude is simply a pure QED phase, some of which should be absorbed into the asymptotic wave functions of incoming and outgoing projectiles.

$$S_{\rm QED}^{q_d}=\frac{q_d Ze^2}{4\pi}\left(\frac{1}{r_0}\int_{-\infty}^{-\tau_d(0)}d\tau+\int_{-\tau_d(b)}^{-\infty}\frac{d\tau}{\sqrt{(b+r_0)^2+\tau^2\sin^2\theta}}\right.$$
$$\left.-\int_0^b d\sigma\frac{(\frac{d\tau_d(\sigma)}{d\sigma})\cos(\frac{\theta\sigma}{b})-\frac{\theta}{b}\tau_d(\sigma)\sin(\frac{\theta\sigma}{b})}{\sqrt{(\sigma+r_0)^2+\tau_d^2(\sigma)\sin^2(\frac{\theta\sigma}{b})}}\right),\qquad(3.8)$$

where the first line comes from the parts of the asymptotic past (future) until (from) the Reggeon interaction region, and the second line represents the contribution from the Reggeon exchange domain given by the interval $0\le\sigma\le b$. See Fig. 3. The charge q_u quark trajectory (the upper trajectory) gives a similar contribution,

$$S_{\rm QED}^{q_u}=\frac{q_u Ze^2}{4\pi}\left(\frac{1}{r_0}\int_{\tau_u(0)}^{\infty}d\tau+\int_{\infty}^{\tau_u(b)}\frac{d\tau}{\sqrt{(b+r_0)^2+\tau^2\sin^2\theta}}\right.$$
$$\left.-\int_0^b d\sigma\frac{(\frac{d\tau_u(\sigma)}{d\sigma})\cos(\frac{\theta\sigma}{b})-\frac{\theta}{b}\tau_u(\sigma)\sin(\frac{\theta\sigma}{b})}{\sqrt{(\sigma+r_0)^2+\tau_u^2(\sigma)\sin^2(\frac{\theta\sigma}{b})}}\right).\qquad(3.9)$$

The naive divergences in the first lines in (3.8) and (3.9) are simply either self-energy due to QED interactions inside the asymptotic bound states, or the same divergences in usual QED pure phase of high-energy eikonal scattering. The former is absorbed into the wave functions of incoming/outgoing states, while the latter can be regularized by an IR cutoff which is also related to the definition of asymptotic wave functions. In any case, these divergences are independent of our variational $\tau_{u,d}(\sigma)$ and they are not of importance for our purposes. We simply regularize them by introducing an IR cutoff and replacing $\pm\infty\to\pm\Lambda_{\rm IR}$. Recall that upon analytic continuation to Minkowski signature, we have to replace $\Lambda_{\rm IR}\to i\Lambda_{\rm IR}$.

The total Reggeon-QED action is a sum of (3.2), (3.8), and (3.9), and the variational equations of motion for $\tau_{u,d}(\sigma)$ can easily be obtained from them. One can check that the boundary terms from the variations of second lines in (3.8) and (3.9) nicely cancel with the variations of the first lines in (3.8) and (3.9), so there are no boundary conditions for $\tau_{u,d}(\sigma)$ at $\sigma=0,\ b$; in other words, their values and derivatives at the boundary $\sigma=0,\ b$ are unconstrained. We see in a moment that this is in fact consistent with the fact that the bulk equations of motion we get for $\tau_{u,d}(\sigma)$ are algebraic, and we do not need and should not have any boundary conditions.

The equations of motion for $\tau_{u,d}(\sigma)$ do not mix with each other and we can treat them separately. The equation of motion for $\tau_u(\sigma)$ reads

$$\frac{1}{2\pi\alpha'}\sqrt{1+\frac{\theta^2}{b^2}\tau_u^2(\sigma)}$$
$$-\frac{q_u Ze^2}{4\pi}\frac{(\cos(\frac{\theta\sigma}{b})(\sigma+r_0)+\frac{\theta}{b}\sin(\frac{\theta\sigma}{b})\tau_u^2(\sigma))}{((\sigma+r_0)^2+\tau_u^2(\sigma)\sin^2(\frac{\theta\sigma}{b}))^{\frac{3}{2}}}=0,\qquad(3.10)$$

and the equation for $\tau_d(\sigma)$ is identical with $q_u\to q_d$. It is convenient to perform analytic continuation $\theta\to-i\chi$ at this stage, and the equation of motion becomes upon defining $y(\sigma)\equiv\tau^2(\sigma)$ (we omit subscript u, d without much confusion)

$$\frac{1}{2\pi\alpha'}\sqrt{1-\frac{\chi^2}{b^2}y(\sigma)}$$
$$-\frac{q_u Ze^2}{4\pi}\frac{(\cosh(\frac{\chi\sigma}{b})(\sigma+r_0)-\frac{\chi}{b}\sinh(\frac{\chi\sigma}{b})y(\sigma))}{((\sigma+r_0)^2-\sinh^2(\frac{\chi\sigma}{b})y(\sigma))^{\frac{3}{2}}}=0.\qquad(3.11)$$

This is our master equation to solve for subsequent discussion.

An example of numerical solutions is given in Fig. 4 for $\chi=15$, $Z=100$, $q_u=1$, and $\frac{b}{\sqrt{\alpha'}}=80$, which shows relevant generic features of the solutions for large χ and b. There exist two qualitatively different regions in the distance space $0\le\sigma\le b$ with a small transition region between them around $\sigma=\sigma_c$, where σ_c is given by solving

$$(\sigma_c+r_0)^2=\sinh^2\left(\frac{\chi\sigma_c}{b}\right)y(0),\qquad(3.12)$$

with

$$y(0)=\tau(0)^2=\frac{b^2}{\chi^2}\left(1-\left(\frac{2\pi\alpha' q_u Ze^2}{4\pi r_0^2}\right)\right)^2\equiv\frac{b^2}{\chi^2}\bar{y}(0),\qquad(3.13)$$

being the solution at $\sigma=0$. As we see in Fig. 4, $y(\sigma)$ is nearly constant in the region $0\le\sigma\le\sigma_c$ with the value $y(0)$, and after that it quickly becomes exponentially small. The condition (3.12) marks the point in σ where the denominator in (3.11) with $y(\sigma)\approx y(0)$ becomes 0, and

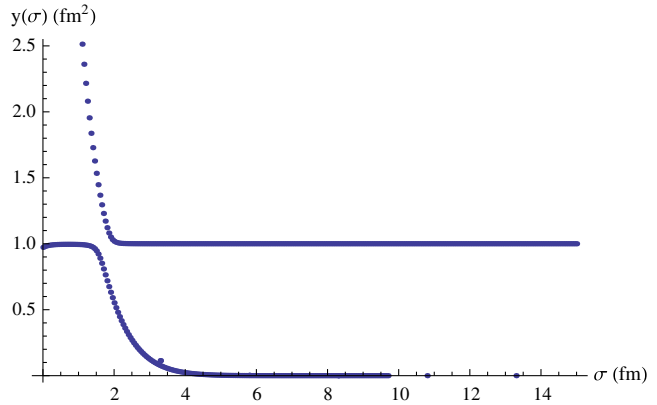

FIG. 4. The numerical solution for (3.11) with $\alpha'=0.036$ fm^2, $r_0=1$ fm, $\frac{e^2}{4\pi}=\frac{1}{137}$, $\chi=15$, $Z=100$, $q_u=1$, and $\frac{b}{\sqrt{\alpha'}}=80$. One has to take the lower branch out of multiple solutions (saddle points). The transition happens when $\sigma_c\approx1.73$ (see the text).

one has a drastic change of behavior of the solution. For large χ and b, one can find an approximate expression for the exponentially small behavior after $\sigma = \sigma_c$,

$$y(\sigma) \approx -\frac{(\frac{2\pi\alpha' q_u Z e^2}{4\pi}(\sigma + r_0)\cosh(\frac{\chi\sigma}{b}))^{\frac{2}{3}}}{\sinh^2(\frac{\chi\sigma}{b})}, \qquad \sigma \gg \sigma_c. \tag{3.14}$$

Note that the solution is highly nonperturbative in QED coupling $\alpha_{\rm EM} = \frac{e^2}{4\pi}$. In fact, there is another branch of solution in the region $\sigma > \sigma_c$ (the upper branch in Fig. 4) which is perturbative in QED interactions,

$$y(\sigma) \approx \frac{b^2}{\chi^2} + \frac{\chi^4}{b^4}\left(\frac{2\pi\alpha' q_u Z e^2}{4\pi}\right)^2 \times \left(\frac{\cosh(\frac{\chi\sigma}{b})(\sigma + r_0) - \frac{b}{\chi}\sinh(\frac{\chi\sigma}{b})}{\sinh^3(\frac{\chi\sigma}{b})}\right)^2, \tag{3.15}$$

and one has to choose the branch (3.14) instead of (3.15), as the former has a smaller value of the real part of the total action $S_{\rm total} = S_{\rm Reggeon} + S_{\rm QED}$. For both branches (3.14) and (3.15), one can easily check that $S_{\rm QED}$ is purely imaginary for $\sigma \geq \sigma_c$, so that it does not play a role in finding the preferred saddle point.[4] The real part of $S_{\rm Reggeon}$ which is simply the area spanned by the string world sheet then prefers a smaller value of $y(\sigma)$, which is the branch (3.14).

It is clear that the region $\sigma > \sigma_c$ with the preferred branch (3.14) makes negligible contribution to the real part of $S_{\rm total}$ that we are interested in. It seems that the same is true for the small transition region around $\sigma \approx \sigma_c$, and the dominant contribution comes from the interval $0 \leq \sigma \leq \sigma_c$ with a nearly constant behavior of the solution $y(\sigma) \approx y(0)$. The contribution to the real part of $S_{\rm Reggeon}$ is therefore

$$\begin{aligned}\mathrm{Re}[S_{\rm Reggeon}] &= \frac{1}{2\pi\alpha'}\int_0^{\sigma_c} d\sigma \int_0^{\tau(\sigma)} d\tau \sqrt{1 - \frac{\chi^2}{b^2}\tau^2} \approx \frac{\sigma_c}{2\pi\alpha'}\int_0^{\tau(0)} d\tau \sqrt{1 - \frac{\chi^2}{b^2}\tau^2} \\ &= \frac{\sigma_c}{4\pi\alpha'}\frac{b}{\chi}\left(\left(\frac{2\pi\alpha' q_u Z e^2}{4\pi r_0^2}\right)\sqrt{1 - \left(\frac{2\pi\alpha' q_u Z e^2}{4\pi r_0^2}\right)^2} + \sin^{-1}\left(\sqrt{1 - \left(\frac{2\pi\alpha' q_u Z e^2}{4\pi r_0^2}\right)^2}\right)\right),\end{aligned} \tag{3.16}$$

using (3.13) for $\tau(0)$. Numerically, $(\frac{2\pi\alpha' q_u Z e^2}{4\pi r_0^2}) \sim 0.132 < 1$ for reasonable values of parameters, such as $\alpha' = 0.036$ fm^2, $Z = 80$, $q_u = 1$, $r_0 = 1$ fm, and $\frac{e^2}{4\pi} = \frac{1}{137}$. It is interesting to note that for extremely large Z such that $(\frac{2\pi\alpha' q_u Z e^2}{4\pi r_0^2}) > 1$, $\tau(0)$ is imaginary and the whole $S_{\rm total}$ becomes purely imaginary. We may interpret this as a complete QED domination over QCD Reggeon amplitudes, which however does not seem to happen in real experiments.

The contribution from $S_{\rm QED}$ to the real part of $S_{\rm total}$ can also be obtained easily, after analytic continuation of $\Lambda_{\rm IR} \to i\Lambda_{\rm IR}$ and assuming $\frac{d\tau(\sigma)}{d\sigma} \approx 0$ over $0 \leq \sigma \leq \sigma_c$,

$$\begin{aligned}\mathrm{Re}[S_{\rm QED}] = &-\frac{q_u Z e^2}{4\pi r_0}\frac{b}{\chi}\sqrt{1 - \left(\frac{2\pi\alpha' q_u Z e^2}{4\pi r_0^2}\right)^2} \\ &+ \frac{q_u Z e^2}{4\pi}\sqrt{1 - \left(\frac{2\pi\alpha' q_u Z e^2}{4\pi r_0^2}\right)^2} \\ &\times \int_0^{\sigma_c} d\sigma \frac{\sinh(\frac{\chi\sigma}{b})}{\sqrt{(\sigma + r_0)^2 - \sinh^2(\frac{\chi\sigma}{b})y(0)}},\end{aligned} \tag{3.17}$$

where the first line comes from the boundary term at $\sigma = 0$.

We are interested in the regime where b is very large (equivalently a small Mandelstam variable t) in units of Fermi. In this case, Eq. (3.12) for σ_c is solved by

$$\sigma_c = C\frac{b}{\chi}, \tag{3.18}$$

where C is a $\mathcal{O}(1)$ numerical number determined by

$$C^2 = \left(1 - \left(\frac{2\pi\alpha' q_u Z e^2}{4\pi r_0^2}\right)^2\right)\sinh^2(C). \tag{3.19}$$

For our previous parameters, $C \approx 0.23$. With this, the integral in the second line of (3.17) can be performed to give

$$\begin{aligned}&\int_0^{\sigma_c} d\sigma \frac{\sinh(\frac{\chi\sigma}{b})}{\sqrt{(\sigma + r_0)^2 - \sinh^2(\frac{\chi\sigma}{b})y(0)}} \\ &= \int_0^{C} d\bar{\sigma} \frac{\sinh\bar{\sigma}}{\sqrt{\bar{\sigma}^2 - \sinh^2\bar{\sigma}\,\bar{y}(0)}},\end{aligned} \tag{3.20}$$

in the $\frac{b}{\chi} \to \infty$ limit, where a dimensionless number $\bar{y}(0)$ was defined previously in (3.13). The above integral is $\mathcal{O}(1)$ in $\frac{b}{\chi}$, of a numerical value 2.74 with our previous parameters. Since the contribution from the Reggeon action

[4]For the branch (3.14), $y(\sigma) < 0$ so that $\tau(\sigma)$ is purely imaginary whereas the denominator in the second line of (3.9) is real, making its contribution to $S_{\rm QED}$ in (3.9) purely imaginary. On the other hand, $\tau(\sigma)$ in the branch (3.15) is real, but the denominator in (3.9) is purely imaginary, and $S_{\rm QED}$ is again purely imaginary.

in (3.16) is quadratic in $\frac{b}{\chi}$, whereas the QED contribution (3.17) is at most linear in $\frac{b}{\chi}$, the former dominates eventually for small t-channel exchanges.

In summary, the leading large b asymptotics of the real part of S_{total} is

$$\text{Re}[S_{\text{total}}] \approx \frac{C}{4\pi\alpha'}\left(\sqrt{\bar{y}(0)(1-\bar{y}(0)}\right) + \sin^{-1}\left(\sqrt{\bar{y}(0)}\right)\frac{b^2}{\chi^2} + \mathcal{O}(b) \approx \frac{1}{4\pi\alpha'(Z)}\frac{b^2}{\chi^2}, \tag{3.21}$$

where C is determined by

$$C^2 - \bar{y}(0)\sinh^2(C) = 0, \tag{3.22}$$

and $\bar{y}(0)$ depends on QED parameters as follows:

$$\bar{y}(0) \equiv 1 - \left(\frac{2\pi\alpha' q_u Z e^2}{4\pi r_0^2}\right)^2. \tag{3.23}$$

This is our main result. One has to add the similar contribution from the lower part of the trajectory with a replacement $q_u \to q_d$. From (3.21) with the use of (2.2) and (2.3), we get the Reggeon amplitude

$$\mathcal{T}^{Ap,A\bar{p}}_{\text{Reggeon}}(s,t) \sim i e^{\alpha'(Z)t(\ln s)^2}, \tag{3.24}$$

and the total cross section

$$\sigma^{Ap,A\bar{p}}_{\text{Reggeon}} \sim \frac{(\log s)^2}{s}. \tag{3.25}$$

This result is different from the usual Reggeon behavior, and now we briefly discuss how it is related to the usual Reggeon as the charge Z is reduced. In Fig. 5 we show the solution of (3.11) with a small charge $Z = 1$. The nontrivial shape solution which plays a key role in our result now comes into contact with the straight horizontal line solution corresponding to the usual Reggeon behavior. What happens is that the second term in (3.11) (equivalently the QED action compared to the QCD action) becomes irrelevant in the small Z limit compared to the first term. Its inclusion in the classical equation of motion (3.11) is no longer justified, since the semiclassical approximation for the second term breaks down. Although it causes the appearance of the nontrivial shape solution, this solution does not play a role of an important saddle point, as the quantum fluctuations are equally important for the path integral of the second term. The dominant action for the meaningful saddle point arises from the first term only in the small Z limit, reproducing the usual Reggeon. We expect the transition from the small Z limit to our large Z limit to be continuous if we consider the full quantum path integral of the world sheet shape $\tau(\sigma)$. More specifically, as Z increases, the second term in (3.11) or the QED action changes from a quantum correction to a semiclassical correction. However, performing the quantum path integral to see this transition goes beyond the scope of our present work.

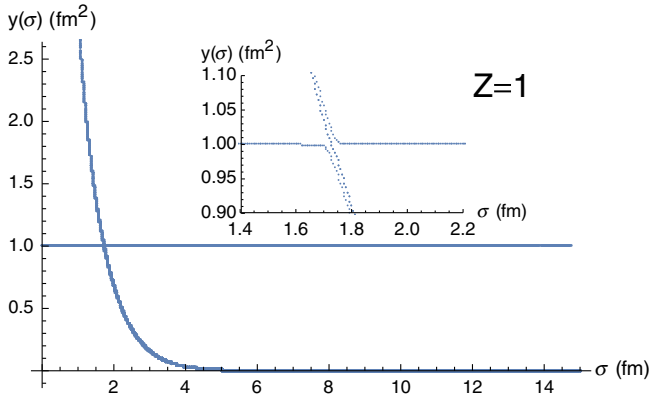

FIG. 5. The numerical solution for (3.11) with a small charge limit $Z = 1$. The solution with a nontrivial shape and the one with the straight horizontal line [for the usual Reggeon $y(\sigma) = b^2/\chi^2$] get closer and closer as Z decreases (see the inset plot). When $Z = 0$, only the latter solution survives.

Let us now briefly discuss possible one loop contributions coming from summing over linearized fluctuations around the above saddle point solution in the path integral of the string world sheet. The one loop determinant of massless fluctuations on the world sheet gives the contribution to the action as

$$S_{\text{one loop}} = \frac{D_\perp}{2}\log\det(\partial^2), \tag{3.26}$$

where $D_\perp$ is the number of massless bosonic degrees of freedom on the string world sheet.[5] In the case of pure Reggeon exchange, the semiclassical string solution has a rectangular shape whose length sizes are b and $\frac{\pi}{2}\frac{b}{\chi}$ [see the solution (2.10)]. In the high-energy limit, $\chi \to \infty$, the shape becomes highly elongated, $b \gg \frac{\pi}{2}\frac{b}{\chi}$, and in this case the one-loop action given above is dominated by the Casimir energy,

$$\frac{D_\perp}{2}\log\det(\partial^2) \approx -\frac{\pi D_\perp}{24}\frac{b}{(\frac{\pi}{2}\frac{b}{\chi})} = -\frac{D_\perp}{12}\chi, \tag{3.27}$$

which enhances the scattering amplitude by a factor

$$\exp\left(-S_{\text{one loop}}\right) = e^{\frac{D_\perp}{12}\chi} = s^{\frac{D_\perp}{12}}. \tag{3.28}$$

[5]World sheet Fermionic fields in general become massive and negligible in the nonsupersymmetric background of holographic QCD [31], indicating a transition from the critical superstring theory to an effective noncritical bosonic string theory [16]. This is a nice revival of the old string theory for QCD.

As it is independent of t, it contributes to the intercept of the Regge trajectory which governs the large s growth of the total cross section. However, in our case of Reggeon interplay with QED photons, we see that our semiclassical string solution has the length sizes of $\sqrt{y(0)} \approx \frac{b}{\chi}$ and $\sigma_c \approx \frac{b}{\chi}$ (since the solution collapses to an exponentially small size beyond $\sigma > \sigma_c$), and the shape remains symmetrical even in the high-energy limit $\chi \to \infty$. In this case, the one-loop action is simply an order unity number, and we would not expect any large χ enhancement from it. Therefore, there would not be a nonzero intercept from the one-loop action, and one can simply take our main result (semiclassical contribution) as the dominant contribution to the full amplitude in the large χ limit. We emphasize that this qualitative change of leading high-energy behavior is due to our nontrivial interplay with the QED photons which is nonperturbative in the QED coupling $\alpha_{\rm EM}$.

In summary, holographic Reggeon exchange scatterings in pp or $p\bar{p}$ collisions, and holographic charged Reggeon exchange in Ap or $A\bar{p}$ at large Z, compare as follows,

$$\mathcal{T}^{pp,p\bar{p}}_{\rm Reggeon}(s,t) \sim is^{\alpha_0+\alpha' t},$$
$$\mathcal{T}^{Ap,A\bar{p}}_{\rm Reggeon}(s,t) \sim ie^{\alpha'(Z)t(\ln s)^2}, \tag{3.29}$$

with $\alpha_0 \approx D_\perp/12 \approx 1/4$ and $\alpha'(Z)$ as defined in (3.21). We show in Fig. 6 the behavior of $\alpha'(Z)$ as a function of Z with our previous parameters, $\alpha' = 0.036$ fm^2, $r_0 = 1$ fm and $q_u = 1$. We note that $\alpha'(Z)$ is a decreasing function of Z with a value of 2–3 for $Z > 80$. Empirically, the Reggeon intercept is $\alpha_0 \approx 0.55$ [1].

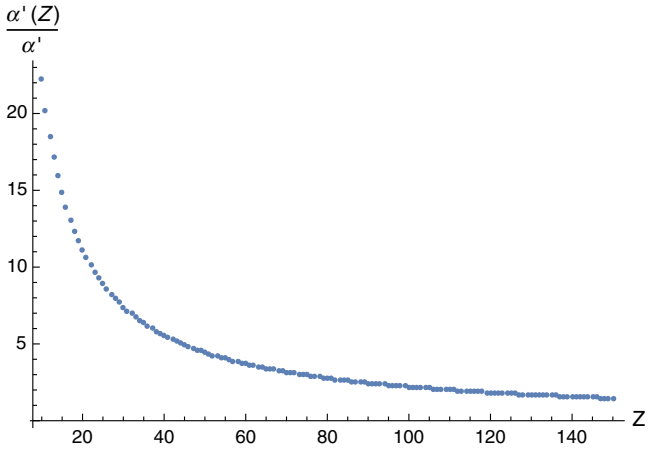

FIG. 6. $\alpha'(Z)$ versus Z for $\alpha' = 0.036$ fm^2, $r_0 = 1$ fm and $q_u = 1$.

IV. CONCLUSIONS

We have found that the large charge of the nucleus in pA collisions modifies the Reggeon slope and its intercept. The effect on the slope is large and leads to a shrinkage of the differential cross section of elastic and diffractive cross sections. Although we have derived this effect in the context of strong coupling holographic QCD, we expect it to be accessible also in perturbative QCD + QED through a pertinent mixing of the parton ladders with photon exchanges. A dedicated pA experiment at the LHC or RHIC using heavy nuclei with large Z is able to test our results.

ACKNOWLEDGMENTS

We thank Yuri Kovchegov, Edward Shuryak and Kirill Tuchin for discussions. This work was supported by the U.S. Department of Energy under Award No. DE-FG-88ER40388.

[1] A. Donnachie and P. V. Landshoff, Total cross sections, Phys. Lett. B **296**, 227 (1992).
[2] E. A. Kuraev, L. N. Lipatov, and V. S. Fadin, The Pomeranchuk singularity in nonabelian gauge theories, Sov. Phys. JETP **45**, 199 (1977); Y. Y. Balitsky and L. N. Lipatov, The Pomeranchuk singularity in quantum chromodynamics, Sov. J. Nucl. Phys. **28**, 822 (1978).
[3] M. Rho, S.-J. Sin, and I. Zahed, Elastic parton-parton scattering from AdS/CFT, Phys. Lett. B **466**, 199 (1999).
[4] R. A. Janik and R. B. Peschanski, Minimal surfaces and Reggeization in the AdS/CFT correspondence, Nucl. Phys. **B586**, 163 (2000).
[5] R. A. Janik and R. B. Peschanski, Reggeon exchange from AdS/CFT, Nucl. Phys. **B625**, 279 (2002).
[6] J. Polchinski and M. J. Strassler, Hard Scattering and Gauge / String Duality, Phys. Rev. Lett. **88**, 031601 (2002).
[7] L. Cornalba, M. S. Costa, and J. Penedones, AdS Black Disk Model for Small-x Deep Inelastic Scattering, Phys. Rev. Lett. **105**, 072003 (2010); L. Cornalba, M. S. Costa, J. Penedones, and P. Vieira, From fundamental strings to small black holes, J. High Energy Phys. 12 (2006) 023.
[8] R. C. Brower, J. Polchinski, M. J. Strassler, and C.-I. Tan, The Pomeron and gauge/string duality, J. High Energy Phys. 12 (2007) 005.
[9] L. F. Alday and J. M. Maldacena, Gluon scattering amplitudes at strong coupling, J. High Energy Phys. 06 (2007) 064.

[10] Y. Hatta, E. Iancu, and A. H. Mueller, Deep inelastic scattering off a Script $\mathcal{N} = 4$ SYM plasma at strong coupling, J. High Energy Phys. 01 (2008) 063; Deep inelastic scattering at strong coupling from gauge/string duality: the saturation line, J. High Energy Phys. 01 (2008) 026.

[11] J. L. Albacete, Y. V. Kovchegov, and A. Taliotis, DIS on a large nucleus in AdS/CFT, J. High Energy Phys. 07 (2008) 074; DIS in AdS , AIP Conf. Proc. **1105**, 356 (2009).

[12] E. Barnes and D. Vaman, Massive quark scattering at strong coupling from AdS/CFT, Phys. Rev. D **81**, 126007 (2010).

[13] R. Nishio and T. Watari, High-energy photon-hadron scattering in holographic QCD, Phys. Rev. D **84**, 075025 (2011).

[14] M. Giordano and R. Peschanski, Reggeon exchange from gauge/gravity duality, J. High Energy Phys. 10 (2011) 108.

[15] M. Giordano, R. Peschanski, and S. Seki, Eikonal approach to $N = 4$ SYM Regge amplitudes in the AdS/CFT correspondence, Acta Phys. Pol. B **43**, 1289 (2012).

[16] G. Basar, D. E. Kharzeev, H.-U. Yee, and I. Zahed, Holographic Pomeron and the Schwinger mechanism, Phys. Rev. D **85**, 105005 (2012).

[17] A. Stoffers and I. Zahed, Holographic Pomeron: saturation and DIS, Phys. Rev. D **87**, 075023 (2013).

[18] A. Watanabe and K. Suzuki, Transition from soft to hard Pomeron in the structure functions of hadrons at small x from holography, Phys. Rev. D **86**, 035011 (2012).

[19] A. Stoffers and I. Zahed, Diffractive and deeply virtual Compton scattering in holographic QCD, arXiv:1210.3724.

[20] A. Stoffers and I. Zahed, Holographic Pomeron and entropy, Phys. Rev. D **88**, 025038 (2013); Y. Qian and I. Zahed, Stringy pomeron: Entropy and shear viscosity, arXiv:1211.6421.

[21] E. Shuryak and I. Zahed, High multiplicity pp and pA collisions: Hydrodynamics at its edge and stringy black hole, Phys. Rev. C **88**, 044915 (2013).

[22] Y. Qian and I. Zahed, A stringy (holographic) Pomeron with extrinsic curvature, Phys. Rev. D **92**, 085012 (2015).

[23] Y. Qian and I. Zahed, Stretched string with self-interaction at high resolution: Spatial sizes and saturation, Phys. Rev. D **91**, 125032 (2015).

[24] E. Shuryak and I. Zahed, New regimes of the stringy (holographic) Pomeron and high-multiplicity pp and pA collisions, Phys. Rev. D **89**, 094001 (2014); T. Kalaydzhyan and E. Shuryak, Self-interacting QCD strings and string balls, Phys. Rev. D **90**, 025031 (2014); T. Kalaydzhyan and E. Shuryak, Collective interaction of QCD strings and early stages of high multiplicity pA collisions, Phys. Rev. C **90**, 014901 (2014).

[25] Y. Qian and I. Zahed, Stretched string with self-interaction at the Hagedorn point: Spatial sizes and black holes, Phys. Rev. D **92**, 105001 (2015).

[26] I. Heemskerk, J. Penedones, J. Polchinski, and J. Sully, Holography from Conformal Field Theory, J. High Energy Phys. 10 (2009) 079.

[27] M. Froissart, Asymptotic behavior and subtractions in the Mandelstam representation, Phys. Rev. **123**, 1053 (1961).

[28] D. J. Gross and P. F. Mende, The high-energy behavior of string scattering amplitudes, Phys. Lett. B **197**, 129 (1987).

[29] O. Nachtmann, Considerations concerning diffraction scattering in quantum chromodynamics, Ann. Phys. (N.Y.) **209**, 436 (1991).

[30] E. Meggiolaro, High-energy scattering, and Euclidean-Minkowskian duality, arXiv:0709.1332; M. Giordano and E. Meggiolaro, Euclidean-Minkowskian duality of Wilson-loop correlation functions, eCONF C 0906083, 31 (2009).

[31] Y. Kinar, E. Schreiber, J. Sonnenschein, and N. Weiss, Quantum fluctuations of Wilson loops from string models, Nucl. Phys. **B583**, 76 (2000).